Eur Biophys J (2006) 35: 439–445
DOI 10.1007/s00249-006-0051-0

ARTICLE

**Roberto Piazza · Matteo Pierno · Sara Iacopini
Palma Mangione · Gennaro Esposito
Vittorio Bellotti**

Micro-heterogeneity and aggregation in β_2-microglobulin solutions: effects of temperature, pH, and conformational variant addition

Received: 13 October 2005 / Revised: 20 January 2006 / Accepted: 7 February 2006 / Published online: 7 March 2006

Abstract We show that β_2-microglobulin solutions in physiological conditions contain a tiny fraction of aggregates, which can hardly be filtered out and tend to re-form spontaneously. At physiological pH the fractional amount and size distribution of the latter aggregates do not depend on temperature. Conversely, in the pH range typical of the peri-articular tissue acidosis that often occurs in hemodialysis, temperature increase leads to fast and irreversible growth of the aggregates. Quite similar, but strongly enhanced aggregation effects can be induced even in physiological conditions by adding a very small amount of ΔN6, a naturally occurring truncated isoform of β_2-m known to promote fibrillogenesis.

Introduction

A large number of severe human pathologies, ranging from Alzheimer's and Parkinson's diseases to familial polyneuropathy and cardiomiopathy, are known to be induced by protein aggregation into large, organized structures known as amyloid fibrils (Merlini and Bellotti 2003). All these diseases, in spite of their manifold clinical aspects, bear in common the accumulation of fibrils in one or more types of tissue, leading to systemic disorder. Dialysis-related amyloidosis (DRA), involving the amyloid deposition of plasmatic β_2-microglobulin (β_2-m), represents an inescapable complication of all dialytic methods making up for chronic renal failure. In such substitutional procedures β_2-m reaches a plasma concentration that is 20–50 times higher than its physiological level, and in more than 90% of the patients undergoing long-term dialysis, β_2-m amyloid fibrils start accumulating after a time lag of a few years in collagen-rich tissues such as bones, ligaments and sinovia, leading to clinical manifestations such as carpal tunnel syndrome, destructive arthropathy, and pathological bone fractures (Drueke 2000).

Hemodialysis is associated with systemic effects comparable to an inflammatory reaction: in fact the interaction between the blood and the dialysis membranes primes the activation of mononuclear cells leading to the production of inflammatory cytokines. The extent of activation is dependent on the dialyzer material used and is considered as an index of biocompatibility. Cytokines, such as interleukin-1 (IL-1), tumor necrosis factor-α (TNF-α), and IL-6, may induce an inflammatory state that acts as an underlying pathophysiologic event in hemodialysis-related acute manifestations, such as temperature increase and hypotension (Pertosa et al. 2000). Control of temperature is a key issue in the dialytic procedure because even independently from the inflammatory effect, the patient temperature tends to increase (Schwalbe et al. 1997). Another crucial side effect of hemodialysis is metabolic acidosis, always requiring medical correction (Kovacic et al. 2003). In the course of inflammation, pH reduction can be very significant in joints, especially in the presence of arthritis and high leukocyte count in the articular fluid (Ward and Steigbigel 1978).

Among the different questions related to fibrillogenesis, the dependence of fibril growth on the solution chemico-physical state and the role played by the solution micro-heterogeneity (possibly triggered by the presence of conformational variants) in promoting aggregation, take on a special role. A number of factors favoring β_2-m fibrillar conversion in vitro have been identified. Connors et al. (1985) have shown that incubation of highly concentrated β_2-m for 5–6 days at

R. Piazza (✉) · M. Pierno · S. Iacopini
Dipartimento di Ingegneria Nucleare, Politecnico di Milano, via Ponzio 34/3, 20133, Milano, Italy
E-mail: roberto.piazza@polimi.it

P. Mangione · V. Bellotti
Laboratorio di Biotecnologia IRCCS Policlinico San Matteo e Dipartimento di Biochimica, Universitá di Pavia, Via Taramelli, 27100, Pavia, Italy

G. Esposito
Dipartimento di Scienze e Tecnologie Biomediche, Universitá di Udine, P.le Kolbe 4, 33100, Udine, Italy

physiological pH and $T = 20°C$ leads, in addition to extensive amorphous aggregation, to the formation of regular fibrils, while rapid aggregation at very low pH has been observed both in the presence (Naiki et al. 1997) and in the absence (McParland et al. 2000) of natural fibril nuclei. Yet, so far no systematic study exists on the effects of temperature on β_2-m aggregation, in particular as a function of the solution pH, which tunes electrostatic effects on the protein structure. Incorrect protein folding has been recognized in many cases as responsible for the formation of fibrillar aggregates (Dobson 1997). Concerning β_2-m, the rapid elongation of fibril seeds in the presence of wild-type (WT) β_2-m conformers, populating the slow phase of the refolding pathway, highlights the role played by the partially folded protein in the genesis of amyloid fibrils (Chiti et al. 2001). In addition, a truncated species of β_2-m lacking the 6 N-terminal residues (ΔN6 β_2-m), which is normally present in natural fibrils, can self-aggregate and make fibrils even in neutral pH conditions (Esposito et al. 2000). A final question is whether fibrils grow from protein monomers associating through a simple monomer-aggregate binding kinetics, or if their nucleation requires 'precursor' aggregates acting as natural 'cradles' for fibril growth (such a behavior has, for instance, been found for Alzheimer's A-β peptides (Soreghan et al. 1995; Lomakin et al. 1996). A related mechanism, dubbed nucleated conformational conversion (NCC) has also been proposed for the yeast prion determinant Sup35 (Serio et al. 1996) and recently extended to β_2-m (Corazza et al. 2004).

The main aim of this work is exploiting dynamic light scattering (DLS) to show that, in physiological conditions, β_2-m solutions are intrinsically micro-heterogeneous: indeed, a tiny fraction of aggregates in the 100 nm size range, which can hardly be detected by other investigation methods, is unavoidably present. At physiological pH, the latter aggregates are relatively stable in size and concentration although, even if carefully filtered out, tend to re-form on a time scale of a few days. Yet, when the solution pH falls in the range typical of the tissue acidosis conditions frequently reported in β_2-m amyloid pathologies, a much faster and irreversible growth of the aggregates takes place at physiological temperature. Conversely, no aggregates, and consequently no growth, are observed for a β_2-m recombinant variant that is specifically stabilized against misfolding. Finally, quite similar, but strongly enhanced aggregate growth can be induced even at physiological pH and temperature by adding to WT β_2-m solutions a very small fraction of the recombinant variant ΔN6.

Materials and methods

Protein preparation and purification

Recombinant WT and ΔN6 β_2-m were prepared as previously described (Esposito et al. 2000). The variant obtained by His–Tyr exchange of the 31st residue (henceforth referred to as Tyr31) was obtained by site directed mutagenesis of β_2-m cDNA as recently reported (Rosano et al. 2004). The protein was purified by a combination of gel filtration in 0.05 M phosphate buffer, 6 M GdnHCL in a Sephacryl S-300 column, refolding of the eluted product in 0.1 M phosphate, 1 mM PMSF 2 mM EDTA buffer at pH 7. Refolded β_2-m was then dialyzed in 0.02 M phosphate buffer at pH = 7.5, loaded onto an anion exchange chromatography column (UNO-BioRad), and finally eluted through a NaCl gradient: by increasing the salt concentration from 0.02 to 0.25 M NaCl, β_2-m iso-forms were progressively eluted as single peaks. The purified protein was then extensively dialyzed against distilled H_2O and analyzed by SDS-PAGE and mass spectrometry as previously described (Esposito et al. 2000).

Static and dynamic light scattering

Let us simply recall that, for solutions of monodisperse particles, the time-correlation function (CF) of the scattered field $g(t)$ obtained in a DLS measurement has a simple exponential shape with a decay rate $\Gamma = Dq^2$, where D is the particle diffusion coefficient, $q = (4\pi n/\lambda)\sin(\vartheta/2)$ is the scattering wave-vector, and n is the refractive index of the solution (Berne and Pecora 1976). An estimate of the size of the scattering objects is given by their hydrodynamic radius $R_H = k_B T/6\pi\eta D$, where η is the solvent viscosity, to be interpreted as the radius of an effective sphere with the same diffusion coefficient. For more complex suspensions, $g(t)$ allows reconstructing in principle, via an inverse Laplace transform, the whole size distribution of the scattering particles, although very low-noise data are required to avoid artifacts. An overall description of our setup has been given elsewhere (Piazza et al. 1998). In the present experiment, measurements were taken at $\lambda = 532$ nm using a 70 mW frequency-doubled Nd^+YAG laser. In order to limit the sample amount, we used a rectangular micro-volume (25 µl) flow-through cell. This cell geometry allows measurements to be taken only at a scattering angle $\vartheta = 90°$, which is fully adequate for detecting mesoscopic aggregates and following the early aggregation stages, but precludes a detailed analysis of the form factor of the scattering objects. Full discussion of the growth kinetics at a later stage, requiring measurements taken with a small-angle light scattering setup, will be discussed in a future work. In the present paper, we shall only present a preliminary investigation, aimed at marking out the main features of temperature and pH effects on β_2-m aggregation.

Results

Micro-heterogeneity at physiological pH

We shall first consider DLS results obtained as a function of temperature on WT β_2-m solutions in phosphate

buffers at pH = 7.4. After extensive cell cleaning with filtered buffer, freshly-prepared samples were injected in the cell, kept at $T_0 = 20°C$, via a syringe terminated with 0.2 μm low protein-binding polysulfone membranes. The temperature was then raised in steps and kept fixed for about 1 h for each step, before measuring DLS correlation functions. Figure 1, displaying the DLS data obtained at pH = 7.4, shows that, even at physiological pH, the CFs are far from being simple exponentials: rather, after a first rapid decay, they display a long, slowly decaying 'tail', suggesting the presence of particles much larger than the protein monomer. A first qualitative analysis of the size distribution performed using CONTIN, a standard DLS size-analysis software, reveals indeed the simultaneous presence of small particles, with a typical size of a few nm, together with a small amount of much larger aggregates in the 100 nm size range. However, all correlation functions approximately superimpose on a single curve when plotted as a function of the rescaled time $t^* = (T\,\eta_0/T_0\eta)\,t$, where η_0 is the solvent viscosity at $T_0 = 20°C$, to get rid of the trivial dependence of Brownian diffusion on T and η. At physiological pH, therefore, the fractional amount and the size distribution of the aggregates does not show any meaningful temperature dependence. We also point out that no relevant change in the correlation function is observed when samples are filtered through 0.8 μm instead of 0.2 μm filters (*data not shown*), suggesting that the observed size distribution is an intrinsic property of the aggregates, rather than a maximum value imposed by the filter cutoff.

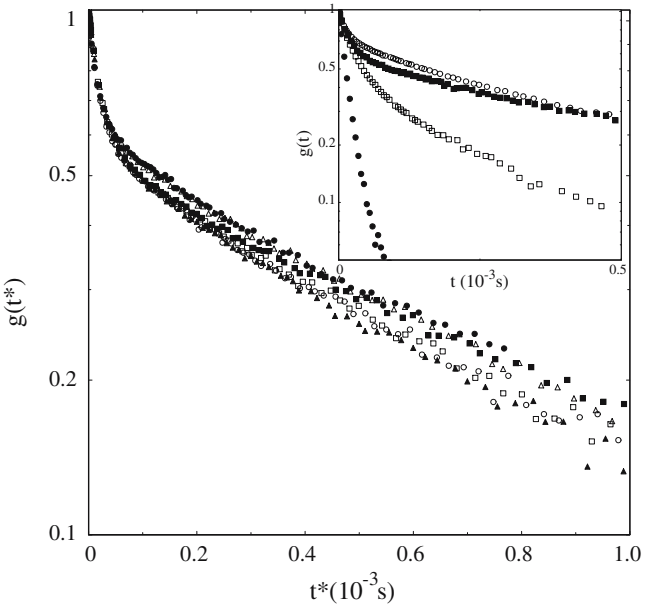

Fig. 1 DLS field correlation functions $g(t)$ for $c = 5$ g/l (0.4 mM) WT β_2-m solutions at pH = 7.4, plotted as a function of the rescaled time t^* defined in the text. The symbols refer to measurements performed at $T = 25°C$ (*open circle*), 30°C (*filled circle*), 38°C (*open square*), 40°C (*filled square*), 50°C (*open triangle*), and 55°C (*filled triangle*). *Inset* Correlation functions at $T = 25°C$ for WT β_2-m solutions before (*open circle*) and after (*filled circle*) extensive filtering with 0.02 μm membranes. Spontaneous aggregate growth upon storage at $T = 25°C$ is shown by the CFs taken 32 (*open square*) and 96 h (*filled square*) after filtering

Dynamic light scattering measurements show therefore that WT β_2-m solutions are, to a certain extent, microscopically heterogeneous. Aggregates are indeed present (albeit in varying amount) regardless of the protein batch storage method (either lyophilization or freezing followed by concentration via ultrafiltration). Preliminary DLS measurements on WT β_2-m directly purified from human amniotic liquid[1] display similar aggregates, proving that the observed micro-heterogeneity is not a peculiar feature of recombinant β_2-m. It is important to point out that the fraction of protein in the aggregate state is anyway very low: a rough estimate, assuming a globular shape for the aggregates gives an upper limit of 10^{-3} of the total monomer content. Therefore, for instance, no significant decrease in NMR signals can be expected as a result of aggregation. One of the crucial questions is whether this micro-heterogeneity simply arises from the presence of a small amount of conformational variants, either naturally present in the expressed protein or artificially generated along the purification process. If this were this the case, and provided that the aggregates are carefully filtered out, no further aggregation should take place. In order to settle this point, we have performed the following experiment. After extensive centrifugation and pre-filtering, a 2 g/l WT β_2-m solution was filtered twice through 0.02 μm Anopore™ nanofilters (Whatman Inc., UK), and fed into the light scattering cell. The upper inset of Fig. 1 shows that this filtration protocol is highly efficient in removing all aggregates: the CF obtained just after filtering (full dots) is indeed almost exponential, yielding a much smaller hydrodynamic radius $R_H \simeq 2.2$ nm, which is consistent with the size of a β_2-m monomer. Yet, when the sample is stored for sufficiently long time at 25°C, aggregates form progressively again: after 4 days, DLS results essentially coincides with those obtained before filtering through the Anopore membrane. This evidence, which should however be supported by a detailed analysis of the aggregate slow-growth kinetics, suggests that aggregation 'seeds' may spontaneously arise in WT β_2-m solution over long time scales.

Thermally-activated aggregate growth at lower pH

As stated in the Introduction, β_2-m amyloid pathologies are often associated with tissue acidosis: for instance, clinically observed values of the local pH in joint fluid for arthritides of various kinds may be as low as 6.3–6.4 (Ward and Steigbigel 1978). It is therefore interesting to inquire about possible pH effects on β_2-m micro-heterogeneity. The DLS results, obtained following the same temperature step increases as in Fig. 1, show indeed that the behavior of WT β_2-m solutions at pH = 6.4 is strik-

[1] Courtesy of M. Galliano, data not shown.

ingly different. As shown in Fig. 2, changes in the CFs are found to be rather modest up to $T \simeq 38°C$. However, by further increasing T, a rapid and dramatic increase of both the total scattering intensity and of the relative contribution of the 'slow' component is observed. While the relative fraction and the size distribution of the aggregates observed at physiological pH do not essentially depend on temperature, these results suggest that acidosis condition triggers the onset of a rather fast and extensive aggregation process. A very simplified analysis of temperature effects on the latter can be obtained by fitting the correlation functions as a double exponential

$$g_1(t) = (1-f)\exp(-\Gamma_m t) + f\exp(-\Gamma_{agg} t), \quad (1)$$

where Γ_m is the decay rate associated with monomers having a hydrodynamic radius R_m, and Γ_{agg} is the average decay rate of the aggregates yielding an hydrodynamic radius R_{agg}. Figure 3 shows that both R_{agg} and the fractional contribution f of the slowly decaying component to $g(t)$ display a rapid increase as a function of T, which can be tentatively fitted as

$$\begin{aligned} \tfrac{R_{agg}-R_0}{R_0} &= \Delta_R \exp(k_R T) \\ \tfrac{f-f_0}{f_0} &= \Delta_f \exp(k_f T), \end{aligned} \quad (2)$$

where R_0 and f_0 are the hydrodynamic radius and the fractional contribution at $T_0 = 20°C$. Albeit this should be considered just as empirical fit, it is interesting to notice that both the amplitudes ($\Delta_R = 4.4\times10^{-2}$, $\Delta_f = 4.5\times10^{-2}$) and the exponential constants ($k_R = 0.11°C^{-1}$, $k_f = 0.10°C^{-1}$) attain very similar values.

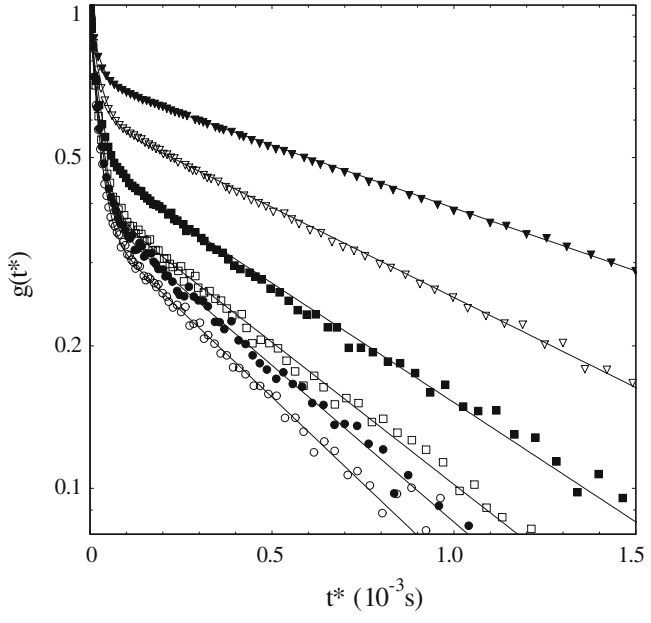

Fig. 2 DLS field correlation functions $g(t)$ for WT β_2-m solutions at pH = 6.4 obtained at $T = 25°C$ (*open circle*), 30°C (*filled circle*), 38°C (*open square*), 40°C (*filled square*), 50°C (*open inverted triangle*), and 55°C (*filled inverted triangle*). *Full lines* are double-exponential fits according to Eq. 1

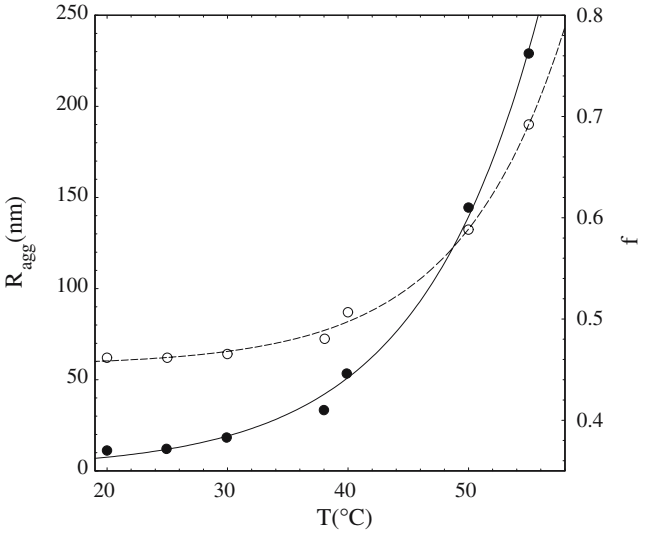

Fig. 3 Temperature dependence (at pH = 6.4) of the aggregate contribution f to $g(t)$ (*filled circle*, *right axis*) and of the average aggregate radius R_{agg} (*open circle*, *left axis*). *Lines* are fits according to Eq. 2

The strong sensitivity on pH of aggregate growth is further emphasized by the results shown in Fig. 4, which shows the temperature dependence of the aggregate radius obtained at three different pH values. In particular, we can notice that at pH = 6.2 aggregates grow very fast even at physiological temperature. We finally point out the observed aggregation process is fully irreversible: albeit growth is quenched by bringing the solution back to low temperature, no aggregate dissolution is indeed observed.

Comparison with other β_2-m variants

The distinctive behavior of WT β_2-m, and its possible relation with a weak propensity to unfolding, is further highlighted by a comparison with the behavior of Tyr31, which is known to be significantly more stable than the WT variant (Rosano et al. 2004). The main body of Fig. 5 shows that, for $25°C < T < 45°C$, the correlation functions obtained in the same conditions of Fig. 2 display no sign of large aggregates, and essentially coincide with the CF obtained for WT β_2-m after filtering with Anopore 0.02 μm filters.

The striking difference between WT and Tyr31 behavior is further marked out in the inset, where the intensity I_S of the light scattered by the two variants at $\vartheta = 90°$ is reported as a function of concentration c (notice that data are taken at much lower concentration values than in DLS measurements). While the linear behavior of I_S for Tyr31 yields a constant average molecular weight, WT β_2-m shows a larger slope even in the very dilute limit, and possibly a further increase of M_W around 30–40 μg/ml (2.5–3.5 μM), which may correspond to a stronger tendency to aggregation taking place beyond a finite concentration threshold. Since the

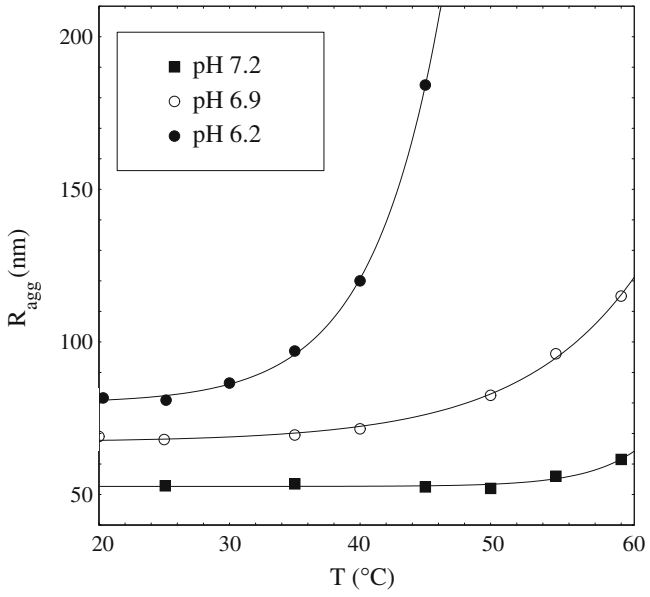

Fig. 4 Temperature dependence of the aggregate hydrodynamic radius at three different pH values, fitted according to Eq. 2

latter range compares rather well with the enhanced β_2-m concentration values observed in β_2-m hemodialysed patients, this finite concentration effect may be of particular interest.

Conversely, the presence of even a small fraction of the natural variant ΔN6, known to have a high propensity to form fibrils around physiologic pH (Esposito et al. 2000), has a dramatic effect on WT β_2-m aggregation. Pure ΔN6 shows such a spontaneous tendency to aggregation that pre-filtering through Anopore^{TM} membranes is hardly feasible. Therefore, to get preliminarily rid of spontaneous WT aggregates, ΔN6 insertion was performed as follows. A pure WT β_2-m solution (pH = 7.4) was fed through 0.02 μm membranes into a much larger volume (1 ml) cell. Small volumes of a precentrifuged ΔN6 solution (up to a maximum of 50 μl, corresponding to a ΔN6 relative concentration of 2.5%) were then progressively injected into the cell via a microvolume Hamilton syringe, and DLS correlation functions measured at $T = 25$°C just after mixing. Figure 6 shows that DLS correlation functions display the presence of a large amount of aggregated β_2-m even at the lowest amount (0.5% of the total protein concentration) of added ΔN6. In Fig. 6, full lines are fits according to Eq. 1 fixing Γ_m to the value obtained for pure β_2-m, which allows extracting the relative contribution f of the aggregates to the total scattering intensity (shown in the inset).

Discussion

Notwithstanding the extensive studies in vitro discussed in the introductory section, the links between β_2-m amyloid conversion in vivo and the physiopathologic conditions associated to hemodialysis are still very poorly understood. The evidence we have reported in this study might represent a step towards understanding

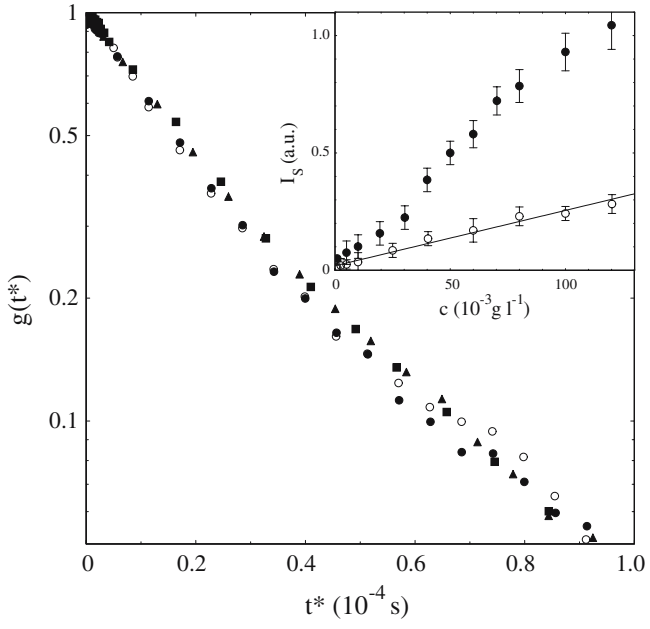

Fig. 5 *Main body* DLS field correlation functions for the Tyr31 variant of β_2-m at $c = 5$ g/l and pH = 6.45, obtained at $T = 25$°C (*filled circle*), 30°C (*filled triangle*), and 45°C (*filled square*), compared to the CF for WT β_2-m at 20°C filtered with 0.02 μm filters (*open circle*). *Inset* Scattered intensity versus concentration for WT (*filled circle*) and Tyr31 (*open circle*) β_2-m solutions

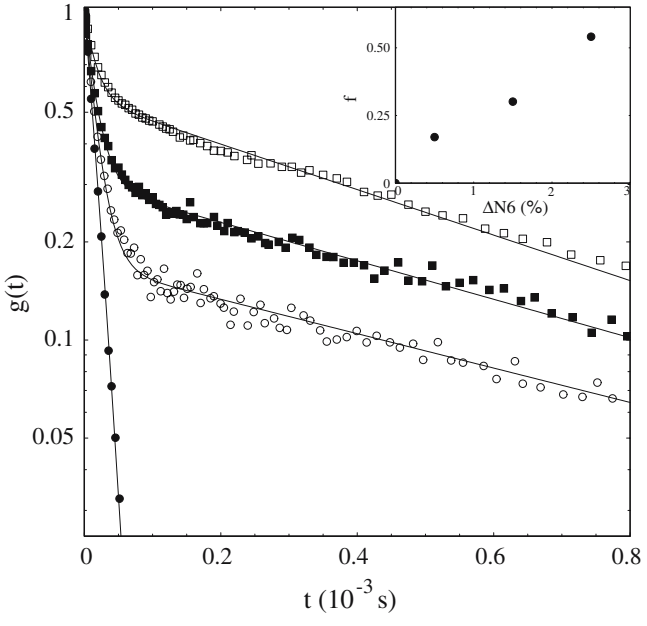

Fig. 6 DLS correlation functions at $T = 25$°C for wild-type β_2-m, pre-filtered with 0.02 μm membranes(*filled circle*), and after the addition of 0.5% (*open circle*), 1.5% (*filled square*), and 2.5% (*open square*) ΔN6 variant. *Inset* Aggregate fractional contribution f to the total scattered intensity

the molecular basis for the well-known inverse correlation between 'biocompatibility' of the hemodialytic procedure and risk of amyloid complication. We have shown that, in physiological conditions, β_2-m displays a spontaneous propensity to associate into large aggregates that elude detection by conventional biochemical methods, but are easily detected by DLS. The occurrence of nucleated oligomeric β_2-m was already suggested on the basis of NMR studies (Corazza et al. 2004). Yet, DLS data show that spontaneous β_2-m aggregation proceeds well beyond the formation of small oligomers, and rather leads to the formation of mesoscopic aggregates. NMR data and other analytical evidence also suggest that β_2-m oligomerization is strongly enhanced for the truncated protein species ΔN6. Consistently, the present data show that the addition of tiny amounts of ΔN6 to WT β_2-m rapidly leads to the formation of large aggregates, demonstrating a seeding capacity of this species in promoting β_2-m aggregation. Our results also suggest that a pathological enhancement of β_2-m concentration may be a factor promoting aggregation. Aggregation seems indeed stronger when the protein concentration reaches values that are easily exceeded in the solvent surrounding the collagen-rich structures that represent the molecular target of β_2-m amyloidosis.

However, the most significant evidence put forward by the present work is probably the strong dependence of β_2-m spontaneous association on pH and temperature. In particular, we have shown that two commonly occurring conditions in chronic hemodialysis, such as fever beyond 38°C and metabolic acidosis or arthritis, may concur to yield a dramatic increase of the number and size of β_2-m aggregates. The observed strong temperature dependence, suggesting an entropic origin of the aggregation process (possibly related to hydrophobic effects), further supports a close relation between aggregation and β_2-m partial unfolding (Chiti et al. 2001; Esposito et al. 2000; Corazza et al. 2004). Enhancement of aggregation in acidic conditions is moreover consistent with the key role played by Hys residues in the folding stability and dynamics of β_2-m (Corazza et al. 2004; Rosano et al. 2004; Villanueva et al. 2004; Verdone et al. 2002). In particular, the pK_a shift of His31 side chain, from 4.17, when β_2-m is bound to the MHCI complex, to 5.4 ± 0.5 for the isolated protein in solution (Corazza et al. 2004) provides the chemical mechanism to destabilize electrostatically the packing of the region encompassing His31 with the N-terminal edge of the sequence, and to trigger the amyloid transformation cascade (Rosano et al. 2004; Verdone et al. 2002). Conversely, when Hys31 is missing, as in the Hys31Tyr variant, no aggregation is observed upon slight pH lowering.

A final important question concerns the specific role played by the presence of spontaneous nanoscale aggregates on β_2-m fibrillogenesis in vivo. It is tempting to suggest that these aggregates, representing local protein reservoirs, may act as 'seeds' for fibril nucleation. This *ansatz* is further supported by the observed strongly cooperative nature of the aggregation process: indeed, the presence of already aggregated protein triggers further β_2-m monomer association. β_2-m aggregates may therefore act as natural 'cradles' for fibril nucleation. Yet, the specific path that leads from the observed unstructured aggregates to the formation of amyloid fibrils in vivo is still unraveled. As a matter of fact, in our experiments we have never observed the formation of regular fibrils, which would be easily detectable by polarized microscopy. Conversely, the deposit that progressively builds up at the cell bottom shows little birefringence by polarized microscopy inspection (possibly ascribable to multiple scattering effects).[2] The situation in vivo may, however, be very different: recently, Relini et al. (in preparation) have observed that globular β_2-m aggregates spontaneously restructure into amyloid fibrils only in the presence of a suitable substrate, like for instance collagen or polylisine (A. Relini et al., in preparation). The presence of amorphous pre-fibrillar aggregates could anyway have a direct biological effect on target cells in vivo. It has indeed been extensively shown that oligomers of amyloidogenic peptides (Lambert et al. 1995) and proteins (Olofsson et al. 2002) can play a direct toxic effect in vitro on target cells, while cytotoxic activity has been already attributed to β_2-m, which may induce cell apoptosis at large enough dosage (Mattson and Goodman 1995; Gordon et al. 2003). Further and more extensive investigation is, however, needed in order to fully assess this crucial point.

Acknowledgements This work has been supported by grants from the Italian Ministries of Health (Grant n.08920301) and of Instruction, University, and Research (MIUR, PRIN 2003 n.2003051399 and FIRB RBNEO1S29H).

References

Berne A, Pecora R (1976) Dynamic light scattering. Wiley, New York

Chiti F, De Lorenzi E, Grossi S, Mangione P, Giorgetti S, Caccialanza G, Dobson CM, Merlini G, Ramponi G, Bellotti V (2001) J Biol Chem 276:46714–46721

Connors LH, Shirahama T, Skinner M, Fenves A, Cohen AS (1985) Biochem Biophys Res Commun 13:1063–1068

Corazza A, Pettirossi F, Viglino P, Verdone G, Garcia J, Dumy P, Giorgetti S, Mangione P, Raimondi S, Stoppini M, Bellotti V, Esposito G (2004) J Biol Chem 279:9176–9189

Dobson CM (1997) Nature 426(6968):884–890

Drueke TB (2000) Nephrol Dial Transplant 15:17–24

Esposito G, Michelutti R, Verdone G, Viglino P, Hernandez H, Robinson CV, Amoresano A, Dal Piaz F, Monti M, Pucci P, Mangione P, Stoppini M, Merlini G, Ferri G, Bellotti V (2000) Protein Sci 5:831–845

Gordon J, Wu CH, Rastegar M, Safa AR (2003) Int J Cancer 103:316–327

[2]Direct check of optical anisotropy effects in the precursor aggregates by depolarized light scattering is unfortunately precluded by the strong refractive index mismatch between β_2-m and water, making the coherent scattering contribution strongly predominant over depolarized scattering, even if it were present (Berne and Pecora 1976).

Kovacic V, Roguljic L, Kovacic V (2003) Am J Nephrol 23:158–164
Lambert MP, Barlow AK, Chromy BA, Edwards C, Freed R, Liosatos M, Morgan TE, Rozovsky I, Trommer B, Viola KL et al (1995) Proc Natl Acad Sci USA 95:6448–6453
Lomakin A, Chung DS, Benedek GB, Kirkschner DA, Teplow DB (1996) Proc Natl Acad Sci USA 93:1125–1129
Mattson MP, Goodman Y (1995) Brain Res 676:219–224
McParland VJ, Kad NM, Kalverda AP, Brown A, Kirwin-Jones P, Hunter MG, Sunde M, Radford SE (2000) Biochemistry 39:8735–8746
Merlini G, Bellotti V (2003) N Engl J Med 349:583–596
Naiki H, Hashimoto N, Suzuki S, Kimura H, Nakakuki K, Gejyo F (1997) Amyloid Int J Exp Clin Invest 4:223–232
Olofsson A, Ostman J, Lundgren E (2002) Clin Chem Lab Med 40:1266–1270
Pertosa G, Grandaliano G, Gesualdo L, Schena FP (2000) Kidney Int Suppl 76:S104–S111
Piazza R, Peyre V, Degiorgio V (1998) Phys Rev E 58:R2733–R2736
Rosano C, Zuccotti S, Mangione P, Giorgetti S, Bellotti V, Pettirossi F, Corazza A, Viglino P, Esposito G, Bolognesi M (2004) J Mol Biol 335:1051–1064
Schwalbe S, Holzhauer M, Schaeffer J, Galanski M, Koch KM, Floege J (1997) Kidney Int 52:1077–1083
Serio TR, Cashikar AG, Kowal AS, Sawicki GJ, Moslehi JJ, Serpell L, Arnsdorf MF, Lindquist SL (1996) Science 289:1317–1321
Soreghan B, Kosmoski J, Glabe C (1995) J Biol Chem 269:28551–28554
Verdone G, Corazza A, Viglino P, Pettirossi F, Giorgetti S, Mangione P, Andreola A, Stoppini M, Bellotti V, Esposito G (2002) Protein Sci 11:487–499
Villanueva J, Hoshino M, Katou H, Kardos J, Hasegawa K, Naiki H, Goto Y (2004) Protein Sci 13:797–809
Ward TT, Steigbigel RT (1978) Am J Med 64:933–936